The Main Anorthosite Layer of the West-Pana Intrusion, Kola Region: Geology and U-Pb Age Dating

Nikolay Y. Groshev [1,*] and **Bartosz T. Karykowski** [2]

[1] Geological Institute of the Kola Science Center of the Russian Academy of Sciences, 184209 Apatity, Russia
[2] Fugro Germany Land GmbH, 12555 Berlin, Germany; bkarykowski@yahoo.com
[*] Correspondence: nikolaygroshev@gmail.com; Tel.: +8-951-296-2355

Abstract: The West-Pana intrusion belongs to the Paleoproterozoic Fedorova-Pana Complex of the Kola Region in NW Russia, which represents one of Europe's most significant layered complexes in terms of total platinum group element (PGE) endowment. Numerous studies on the age of the West-Pana intrusion have been carried out in the past; however, all published U-Pb isotope ages were determined using multi-grain ID-TIMS. In this study, the mineralized Main Anorthosite Layer from the upper portion of the intrusion was dated using SHRIMP-II for the first time. High Th/U (0.9–3.7) zircons gave an upper intercept age of 2509.4 ± 6.2 Ma (2σ), whereas the lower portion of the intrusion was previously dated at 2501.5 ± 1.7 Ma, which suggests an out-of-sequence emplacement of the West-Pana intrusion. Furthermore, high-grade PGE mineralization hosted by the anorthosite layer, known as "South Reef", can be attributed to (1) downward percolation of PGE-enriched sulfide liquid from the overlying gabbronoritic magma or (2) secondary redistribution of PGEs, which may coincide with a post-magmatic alteration event recorded by low Th/U (0.1–0.9) zircon and baddeleyite at 2476 ± 13 Ma (upper intercept).

Keywords: PGE; South Reef; West-Pana intrusion; Fedorova-Pana Complex; zircon dating; U-Pb

1. Introduction

The West-Pana intrusion represents the central block of the Paleoproterozoic Fedorova-Pana Complex located in the central part of the Kola Peninsula. It hosts several platinum group element (PGE) deposits that are interpreted to represent contact- and reef-style mineralization (Figure 1). The Fedorova-Tundra deposit occurs at the basal contact of the complex [1], whereas the North Kamennik, Kievey, and East Chuarvy deposits [2–4] are located at different stratigraphic levels of the complex and comprise one of Europe's largest PGE resource, exceeding 400 t of precious metals [5,6]. The West-Pana intrusion is the first layered intrusion known in Russia that hosts low-sulfide PGE mineralization at several stratigraphic levels, which share many similarities with the well-known Merensky Reef of Bushveld Complex and the J-M Reef of the Stillwater Complex, respectively [7].

In general, PGE mineralization at West-Pana occurs in two distinct layered horizons, both consisting of interlayered pyroxenite, norite, gabbronorite, and anorthosite. Anorthosites of the Lower Layered Horizon form relatively thin and discontinuous layers and host continuous PGE mineralization known as the "North Reef" [8]. Among the anorthosites of the Upper Layered Horizon, the thickest layer is the "Main Anorthosite Layer" [9], hosting highly discontinuous PGE-rich sulfide mineralization in the its upper two meters, which is referred to as the "South Reef" [10,11].
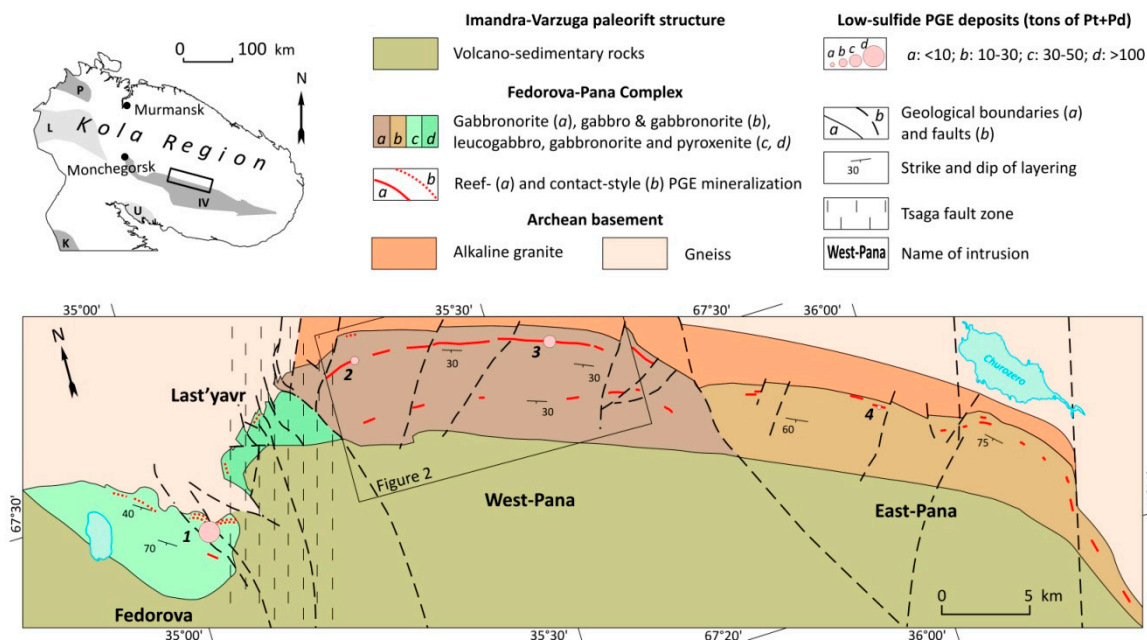
Figure 1. Simplified geological map of the Fedorova-Pana Complex, showing the location of low-sulfide PGE deposits (**1**, Fedorova Tundra; **2**, North Kamennik; **3**, Kievey; **4**, East Chuarvy). Modified after [12]. Proterozoic structures of the predominantly Archean Kola Region (inset): Imandra-Varzuga (IV), Kuolajarvi (K), and Pechenga (P) paleorift structures; Lapland (L) and Umba (U) granulite belts.

It is generally believed that the formation of PGE mineralization in most Russian Paleoproterozoic layered intrusions is related to the long duration of magmatism associated with prolonged igneous activity in response to a long-lived mantle plume affecting the Kola Craton for more than 50 Ma, which is mainly based on ID-TIMS U-Pb age dating [13,14]. This interpretation is generally at odds with the current paradigm of relatively short-lived mantle plume magmatism and the duration of cooling of basaltic magma chambers, such as the Bushveld Complex, which crystallized in less than 1 Ma [15].

The oldest published age for the West-Pana intrusion is 2501.5 ± 1.7 Ma for a gabbronorite from the Lower Layered Horizon [16], whereas the youngest age is 2447 ± 12 Ma for the Main Anorthosite Layer [13]. In this study, we provide new insights into the geology and the petrogenesis of the Main Anorthosite Layer based on recent drilling and U-Pb dating of zircon using SHRIMP-II. The results are discussed in the context of previous age dates from the complex, thus constraining the emplacement and crystallization history of the Fedorova-Pana Complex and anorthosite-hosted PGE mineralization. The study emphasizes the need for more high-precision zircon dating to elucidate the entire emplacement history of the complex.

2. Geological Setting

The Fedorova-Pana Complex includes an almost continuous strip of NW–SE-trending layered intrusions, located at the northern edge of the Imandra-Varzuga paleorift structure (Figure 1). The total extent of the strip is about 90 km in length and up to 6–7 km wide. The northern contact zone of all intrusions is composed of fine-grained gabbroic rocks that intruded the basement lithologies. The rocks in these zones are generally foliated and modified to epidote-amphibolite facies. The southern contact of the complex is defined by a northwest-trending fault with a dip angle of 40–50°, along which younger volcano-sedimentary rocks were thrust onto the complex. The Fedorova-Pana Complex consists of four intrusions, which are from west to east: Fedorova, Last'yavr, West-Pana, and East-Pana (Figure 1). Although all these intrusions are generally presented and explained as a single entity [1,8,16], most researchers believe that each intrusion represents a separate magma chamber with a distinct stratigraphy and formation history [4,17–21].

The West-Pana intrusion is a sheet-like 4 km-thick body, extending for more than 25 km along strike (Figure 2). The magmatic layering dips southwest at an angle of approximately 30–35° [22]. The stratigraphy of West-Pana is rather simple: the lowermost portion is represented by a thin Norite Zone (50 m) that is underlain by a marginal zone comprised of fine-grained gabbronorite, which is often strongly altered due to tectonic activity along the lower intrusion contact. The remainder of the intrusion is essentially unaltered and consists of massive gabbroic rocks of the Gabbronorite Zone except for two distinct horizons: the lower and upper layered horizons. The Lower Layered Horizon (LLH) is located some 600–800 m above the lower intrusion contact and is composed of several cyclic units, consisting of pyroxenite, gabbronorite, leucogabbro, and anorthosite with an average total thickness of 40 m [23]. Significant low-sulfide Pt-Pd mineralization is predominantly concentrated in the second cycle of the LLH, which is referred to as the "North Reef" [24]. Moreover, the LLH and the overlying massive gabbronorites are intruded by late magnetite gabbro [25]. The Upper Layered Horizon (ULH) is situated about 3000 m above the base of the intrusion and consists of two distinct parts with a total thickness of 300 m [26]. The lower part is characterized by a 100 m-thick zone of interlayered norite, gabbronorite, and anorthosite, whereas the upper part consists of cyclically interlayered olivine gabbronorite, troctolite, and anorthosite, which is often referred to as the "Olivine Horizon". The low-sulfide PGE mineralization is associated with both parts of the ULH, but it does not form a continuous ore body. The most significant PGE mineralization is hosted by the "South Reef", which occurs within the Main Anorthosite Layer, representing the thickest anorthosite layer in the lower part of the ULH.
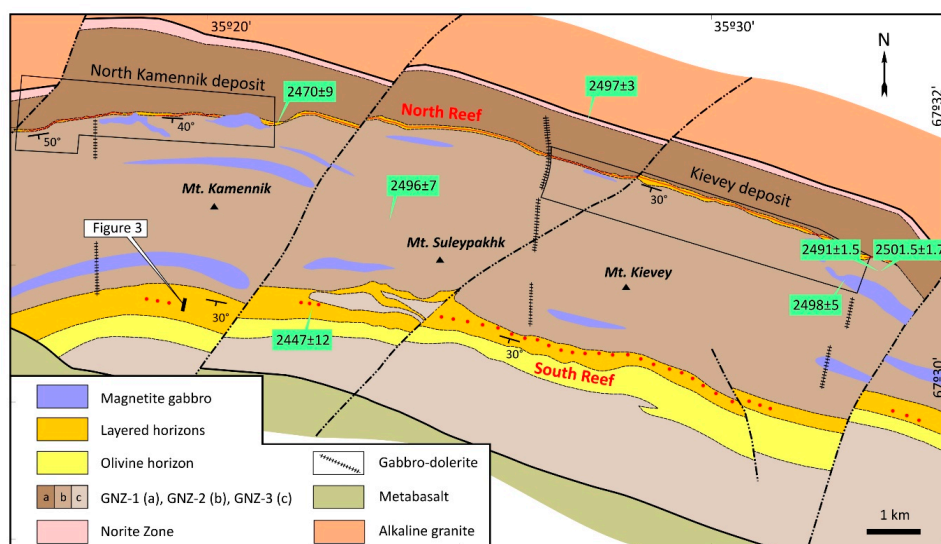
Figure 2. Simplified geological map of the West-Pana intrusion. Published U-Pb ages are shown in green rectangles. Note that the intrusion was explored for PGE mainly along strike of the North and South Reefs, but sub-economic to economic deposits were only discovered in the former. Abbreviations: GNZ, Gabbronorite Zone. Modified after [3].

The 10–17-m-thick Main Anorthosite Layer on the southern slope of Mt. Kamennik can be traced for up to 2 km based on drilling and outcrop mapping. In contrast, the eastern portion of the Main Anorthosite Layer at Mts. Suleypakhk and Kievey has a confirmed strike length of at least 10 km (Figures 2 and 3). The underlying lithology is a medium-grained gabbronorite (Figure 4A), and the contact between the gabbronorite and the anorthosite is gradational (Figure 4B). The overlying unit is composed of medium-grained, sometimes inequigranular gabbronorite that has a sharp contact with the underlying anorthosite (Figure 4C–F). Locally, a discontinuous, 1–2-m-thick norite layer occurs at the base of the overlying gabbronorite. These norites contain traces of PGE mineralization (<0.8 ppm Pd), as well as inequigranular gabbronorites associated with hornfels

xenoliths (Figure 3) [27]. High-grade PGE mineralization with up to 33 ppm Pd is concentrated in the uppermost two meters of the anorthosite layer and is known as the "South Reef" [8,11].
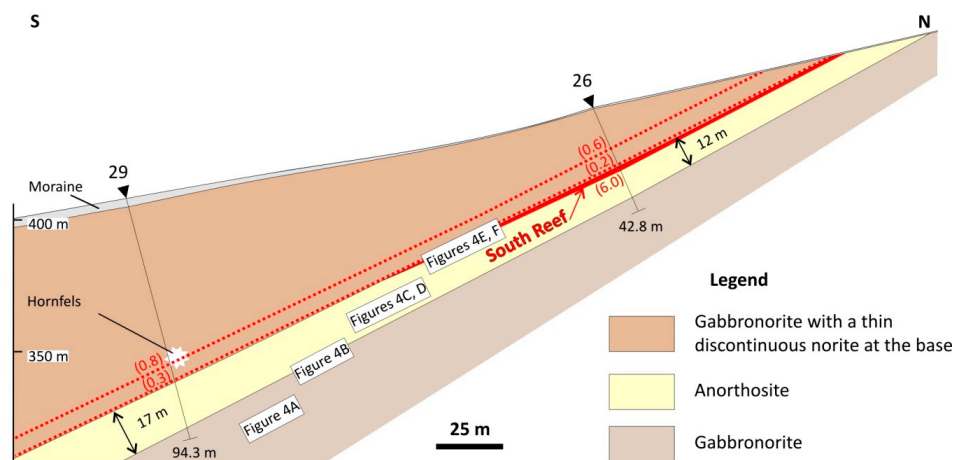
Figure 3. Simplified cross-section of the Main Anorthosite Layer from the West-Pana intrusion based on internal data from JSC Pana. The South Reef is shown as a solid red line, whereas PGE mineralization is indicated by red dotted lines. Note that the hornfels-hosted PGE mineralization (Borehole 29) is traced up-dip in the inequigranular gabbronorites (Borehole 26). Maximum Pd concentrations in drill core samples are shown in parentheses.
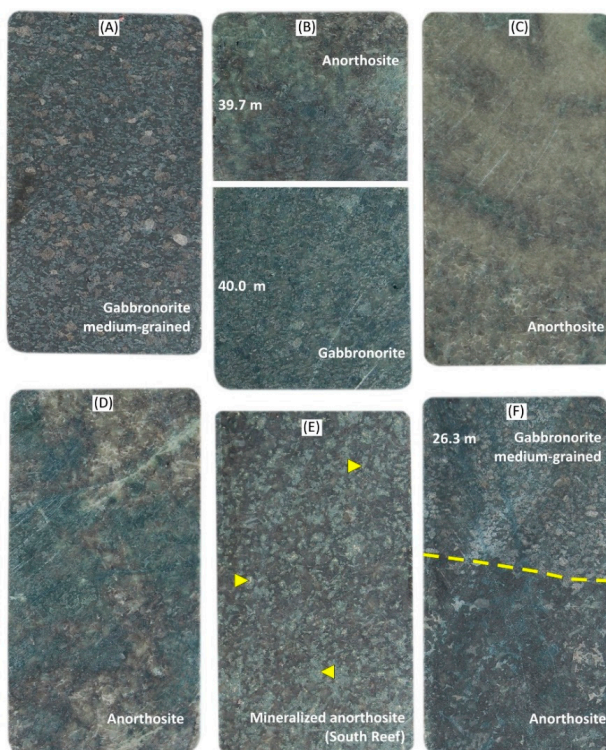
Figure 4. Different rock types from the Main Anorthosite Layer and its host rocks (Borehole 30). (**A**) Medium-grained gabbronorite from the footwall of the Main Anorthosite Layer (depth: 42.15–42.30 m). (**B**) Thirty centimeter-thick gradational lower contact of the Main Anorthosite Layer (depth: 39.7–40.0 m). (**C**) Monomineralic anorthosite (depth: 33.20–33.35 m). (**D**) Mottled anorthosite (depth: 29.45–29.6 m). (**E**) Mineralized anorthosite from the "South Reef". The sample contains 2 ppm Au, 3 ppm Pt, and 33 ppm Pd, respectively. Note the replacement of interstitial minerals by secondary epidote and sulfides (depth: 27.75–27.90 m). (**F**) Sharp upper contact (dashed line) between anorthosite and the overlying medium-grained gabbronorite (depth: 26.30–26.45 m).

These "South Reef" anorthosites are coarse-grained cumulate rocks with a mottled texture, containing some 75–98 vol. % plagioclase, intercumulus quartz, ortho-, and clino-pyroxene, as well as secondary amphibole, biotite, epidote with minor amounts of chalcopyrite, bornite, millerite, pentlandite, pyrrhotite, magnetite, and ilmenite. Accessory minerals include zircon, baddeleyite, apatite, titanite, and rutile. More than three tens PGE and Au minerals occur in the mineralized anorthosite [11,27]. The mottled texture of the anorthosite is defined by the local concentration of plagioclase crystals in distinct areas (Figure 4C), whereas other parts are strongly affected by autometamorphic processes, leading to the complete replacement of the initial intercumulus mineral assemblages by secondary amphibole and epidote (Figure 4D). The mineralized anorthosite contains 2–5 vol. % disseminated sulfide (Figure 4E), mostly hosted by secondary epidote interstitial to cumulus plagioclase (Figure 5A).
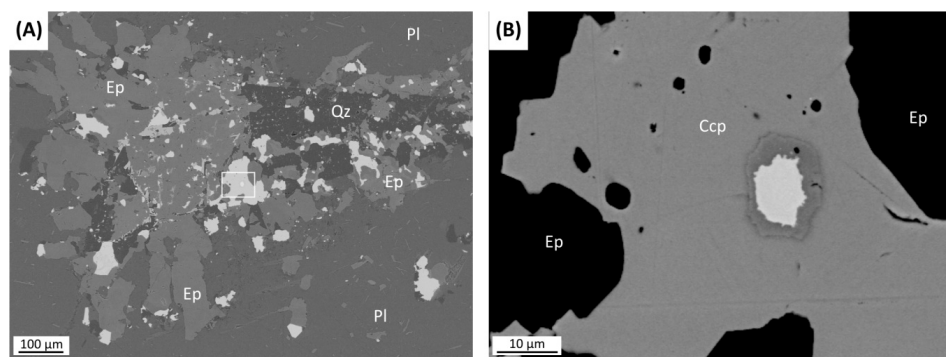
Figure 5. Back-scatter electron images of (**A**) finely-disseminated sulfides (light) intergrown with epidote, replacing the intercumulus space in the mineralized anorthosite and (**B**) baddeleyite rimmed by zircon hosted by chalcopyrite (Ccp). Abbreviations: Ep, epidote; Qz, quartz; Pl, plagioclase.

Moreover, the stratigraphic position of the "South Reef" PGE mineralization appears to be unrelated to changes in the mineral composition of cumulus rock-forming minerals, whereas the position of the "North Reef" coincides with a distinct increase in the anorthite content of plagioclase [9,28,29]. Unlike the barren anorthosite with unzoned plagioclase, the mineralized anorthosites of the "South Reef" are characterized by pronounced zonation of cumulus plagioclase, showing distinct brown rims that have a similar compositions to plagioclase rims from the overlying cumulate [9]. Furthermore, the composition of braggite and vysotskite from the "South Reef" indicates that the crystallization temperature of these minerals is about 750 °C, which is well below the crystallization temperature of these minerals from other deposits across the Fedorova-Pana Complex (830–920 °C) [30]. Thus, several lines of evidence indicate that the low-sulfide PGE mineralization of the "South Reef" is secondary in nature, either post-magmatic or locally remobilized, but the source and processes leading to sulfide concentration in the uppermost portion of the anorthosite layer remain unknown.

3. Materials and Methods

Three drill cores (26, 29, 30) intersecting the Main Anorthosite Layer were used for this study (JSC Pana, 2012–2013). A detailed overview of the petrography and mineral chemistry of the Main Anorthosite Layer is given in [9,11,12,26].

About 30 zircon grains with a size of 50–250 μm were separated from sample BG29 (~10 kg; Borehole 29 in Figure 3) using the methodology described in [31]. The zircon textures were investigated using optical microscopy, cathodoluminescence (CL), and back-scatter electron (BSE) images (Figure 6). The CL and BSE imaging were performed on a CamScan MX2500 scanning electron microscope equipped with a CLI/QUA2 system at the Centre of Isotopic Research of the Russian Geological Research Institute (CIR VSEGEI) in St. Petersburg, Russia.
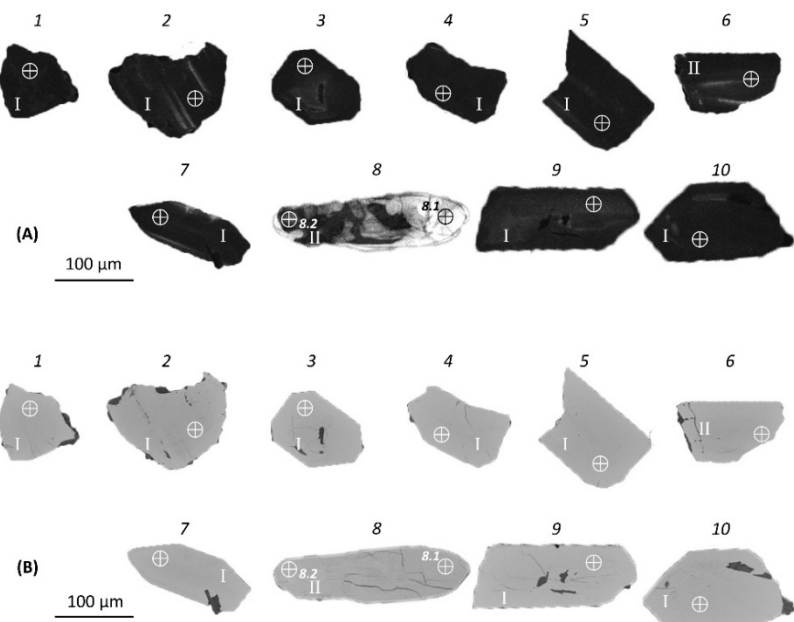
Figure 6. Images of different zircons from Sample BG29. (**A**) Cathodoluminescence (CL) images. (**B**) BSE images. Crosshairs on grains and Arabic numerals correspond to the points of analyses in Table 1; Roman numerals show zircon groups.

The analyses of U-Pb isotope ratios in zircon were carried out on a SHRIMP-II secondary-ion mass spectrometer at CIR VSEGEI using the method outlined in [32,33]. The intensity of the primary molecular oxygen beam was 4 nA; the size of the sampling crater was 20 × 25 μm with a depth of 2 μm. Correction for non-radiogenic Pb was carried out using the measured ^{204}Pb and the modern isotopic composition of Pb from [34]. The data processing was conducted using the software SQUID 1 [35], including concordia age calculation. The analytical results are shown in Table 1.

Table 1. SHRIMP and ID-TIMS U-Pb data for zircon and baddeleyite (bd) from the Main Anorthosite Layer of the West-Pana intrusion. Errors in isotopic ratios and ages are at the 1σ level. Pb$_c$ and Pb* indicate the common and radiogenic lead portions, respectively. The error in standard calibration was 0.51%. Common Pb corrected using measured ^{204}Pb. Abbreviations: D, discordance; Rho, correlation coefficient; nd, no data.

Spot/Fraction Name	^{206}Pb$_c$ (%)	Concentrations/Ratios				^{206}Pb/^{238}U-age (Ma)	^{207}Pb/^{206}Pb-age (Ma)	D (%)	Isotope Ratios						Rho
		U (ppm)	Th (ppm)	Th/U	^{206}Pb * (ppm)				^{207}Pb */ ^{206}Pb *	1σ (%)	^{207}Pb */ ^{235}U	1σ (%)	^{206}Pb */ ^{238}U	1σ (%)	
						SHRIMP data, this study									
1.1	0.01	787	1003	1.32	302	2383 ± 34	2497.0 ± 3.8	5	0.1640	0.22	10.110	1.7	0.4472	1.7	0.992
2.1	0.01	304	310	1.06	119	2416 ± 29	2507.6 ± 6.2	4	0.1650	0.37	10.350	1.5	0.4547	1.5	0.969
3.1	0.05	186	141	0.78	74	2448 ± 30	2506.0 ± 7.9	2	0.1649	0.47	10.500	1.5	0.4618	1.5	0.952
4.1	0.03	444	373	0.87	179	2475 ± 29	2501.3 ± 4.9	1	0.1644	0.29	10.610	1.5	0.4681	1.4	0.980
5.1	0.05	399	1436	3.72	146	2292 ± 46	2497.7 ± 5.5	9	0.1640	0.33	9.660	2.4	0.4270	2.4	0.991
6.1	0.04	210	28	0.14	89	2586 ± 31	2499.6 ± 7.3	−3	0.1642	0.43	11.170	1.5	0.4935	1.5	0.959
7.1	0.10	228	268	1.22	92	2480 ± 30	2511.6 ± 7.2	1	0.1654	0.43	10.700	1.5	0.4691	1.5	0.960
8.1	0.24	29	25	0.87	10	2160 ± 36	2340.0 ± 25.0	8	0.1495	1.50	8.200	2.4	0.3980	1.9	0.794
8.2	0.05	416	120	0.30	116	1818 ± 23	2159.0 ± 14.0	19	0.1346	0.83	6.046	1.7	0.3258	1.4	0.865
9.1	0.06	200	405	2.09	82	2516 ± 30	2513.2 ± 7.7	0	0.1656	0.46	10.900	1.5	0.4775	1.5	0.954
10.1	0.04	371	333	0.93	151	2498 ± 30	2506.4 ± 8.6	0	0.1649	0.51	10.760	1.5	0.4733	1.4	0.942
						ID-TIMS data from [13]									
P6-2	nd	1331	nd	nd	743	nd	2438	nd	nd	nd	9.588	0.5	0.4393	0.5	0.865
P6-3	nd	577	nd	nd	286	nd	2474	nd	nd	nd	8.643	0.5	0.3874	0.5	0.794
P5-bd	nd	396	nd	nd	176	nd	2435	nd	nd	nd	9.548	0.5	0.4380	0.5	0.865
P6-bd	nd	560	nd	nd	259	nd	2443	nd	nd	nd	9.956	0.5	0.4533	0.5	0.794

4. Results of Zircon Imaging and U-Pb SHRIMP Dating

The studied set of zircons is relatively heterogeneous and can be divided into two distinct groups based on age, morphology, texture, and composition (Figure 6). The analytical results of the U-Pb isotope dating are given in Table 1 and plotted in the concordia diagram in Figure 7.
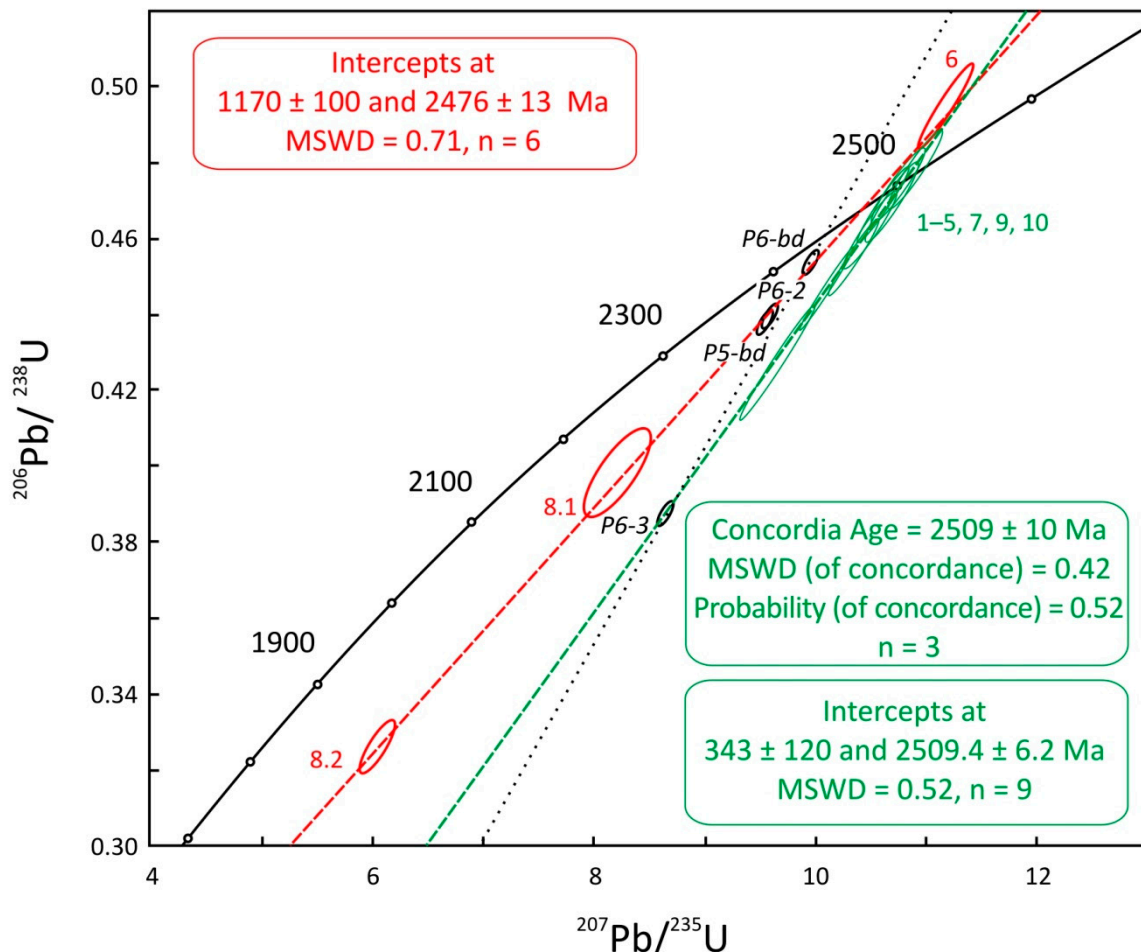
Figure 7. Concordia diagram for zircons separated from sample BG29 (coarse-grained anorthosite) with zircon and baddeleyite data from samples P5 and P6 (italic). Green ellipses show zircon with high Th/U ratios (mainly 0.9–3.7); red ellipses represent zircon with low Th/U ratios (0.1–0.9); black ellipses show zircon and baddeleyite (bd) from [13]. The dotted line shows the discordia exclusively based on ID-TIMS data.

The first group of zircons (eight grains: 1–5, 7, 9, 10) comprises fragments of large columnar crystals, showing a weak zonation in CL images. Most of these zircons have a low discordance (Table 1).Three of them (7, 9, 10) have a discordance close to zeroand plot on the concordia with a calculated age of 2509 ± 10 Ma (including decay constant errors; MSWD = 0.42; concordance probability is 0.52). Three relatively discordant zircon grains of this group (1, 2, 5) together with concordant zircons form a discordia, which includes the ID-TIMS multi-grain zircon analysis P6-3 (Figure 7). This data point was taken from a previous study and represents a zircon from the same lithology [13]. The upper intercept age of the resulting composite discordia (n = 9) is 2509.4 ± 6.2 Ma (MSWD = 0.52), whereas the lower intercept corresponds to an age of 343 ± 120 Ma.

The second group of zircon is represented by two grains (6, 8): the first grain strongly resembles zircon from the first group in terms of morphology and internal texture, but due to its composition, it was included in this group (cf. Th/U ratios in Table 1); the second zircon is elongated with a round shape and shows distinct internal domaining (Figure 6). Figure 7 shows that these Group 2 zircons

form a discordia together with zircon (P6-2) and baddeleyite (P5-bd, P6-bd) from the same rocks analyzed by ID-TIMS in a previous study [13]. The upper intercept age of this composite discordia is 2476 ± 13 Ma (MSWD = 0.71).

5. Discussion

5.1. U-Pb Age of the Main Anorthosite Layer and Crystallization History of the West-Pana Intrusion

The existing U-Pb age of 2447 ± 12 Ma for the Main Anorthosite Layer (Table 2) was determined by multi-grain ID-TIMS on zircon and baddeleyite [13]. Since baddeleyite generally crystallizes as a late-stage mineral in layered intrusions [36], this age was considered to indicate the crystallization age of the anorthosite. Therefore, the Main Anorthosite Layer was interpreted to represent an additional sill-like intrusion that was emplaced some 50 Ma after the crystallization of the West-Pana intrusion [13,37].

Table 2. Published isotope U-Pb rock ages of the Fedorova-Pana Complex.

Intrusions	Rock Type	Age (Ma)	Mineral	References
Fedorova	gabbronorite min.	2485 ± 9	4 Zrn, SD	[38]
	gabbronorite min.	2493 ± 8	4 Zrn, SD	[39]
	orthopyroxenite	2526 ± 6	4 Zrn, SD	[38]
	leucogabbro min.	2518 ± 9	3 Zrn, SD	[39]
	leucogabbro	2515 ± 12	4 Zrn, SD	[39]
	leucogabbro	2516 ± 7	3 Zrn, SD	[38]
	leucogabbronorite	2507 ± 11	6 Zrn, D	[39]
West-Pana	norite	2497 ± 3	4 Zrn, SD	[38]
	gabbronorite	2496 ± 7	3 Zrn, D	[38]
	gabbronorite	2491 ± 1.5	3 Zrn, D	[13]
	gabbronorite	2501.5 ± 1.7	3 Zrn, C	[16]
	gabbro-pegmatite	2470 ± 9	3 Zrn, DC	[40]
	magnetite gabbro	2498 ± 5	3 Zrn, DC	[13]
	anorthosite	2447 ± 12	3 Zrn + 2Bdy, DC	[13]
East-Pana	gabbro	2487 ± 10	4 Zrn, SD	[12]
	gabbro-pegmatite	2464 ± 12	2 Zrn + 2Bdy, SD	[41]

C, concordant zircons; DC, discordant zircons with concordant zircon(s); D, discordant zircons; SD, strongly-discordant zircons; min., mineralized. All errors are reported as 2σ.

Based on the U-Pb SHRIMP-II dating of zircon from the Main Anorthosite Layer, two stages in the formation of the layer can be distinguished: (1) a magmatic stage and (2) a post-magmatic metasomatic stage. The magmatic stage is mainly represented by zircons from the first group and characterized by relatively high Th/U ratio, ranging from 0.9–3.7 (Table 1). Therefore, the calculated concordia age of 2509 ± 10 Ma and the slightly more precise upper intercept age of 2509.4 ± 6.2 Ma most likely represent the actual crystallization age of the anorthosite. In contrast, the second group of zircons has lower Th/U ratios, ranging from 0.1–0.9 (Table 1) and belongs to the post-magmatic metasomatic stage. Consequently, the upper intercept age of 2476 ± 13 Ma records the autometasomatic overprint of the anorthosites. It should be noted that late-stage baddeleyite in these anorthosites is unlikely to be magmatic as it mostly occurs together with secondary amphibole, epidote, and with presumably remobilized sulfide mineralization (Figure 5B), rather than with a typical magmatic interstitial mineral assemblage. This may explain the large difference between the 2509.4 ± 6.2 Ma age determined by SHRIMP-II and the 2447 ± 12 Ma ID-TIMS age for the same lithological unit. A potential mechanism for the autometasomatic overprint of the anorthosites may have been the downward infiltration of residual melts from the overlying gabbronoritic unit (Figure 3).

Geological relationships coupled with U-Pb dating of the Main Anorthosite Layer suggest that the layer crystallized coevally with the adjacent rocks of the ULH, but earlier than the LLH and other rocks from the lower portions of the West-Pana intrusion (Figures 2 and 8). This conclusion is consistent with available age dates from the layered series of the Fedorova intrusion that range from 2526–2507 Ma,

whereas the basal marginal series is younger with 2493–2485 Ma (Table 2), although secondary overprinting may have obscured the actual crystallization ages. Notably, the Main Anorthosite Layer shares many similarities with the Anorthosite zones in the Middle Banded Series of the Stillwater Complex as these anorthosites are older than the underlying rock sequences, which also host the J-M Reef. This was interpreted to suggest an out-of-sequence emplacement of the Stillwater Complex, which could also apply to the Fedorova-Pana Complex [42].
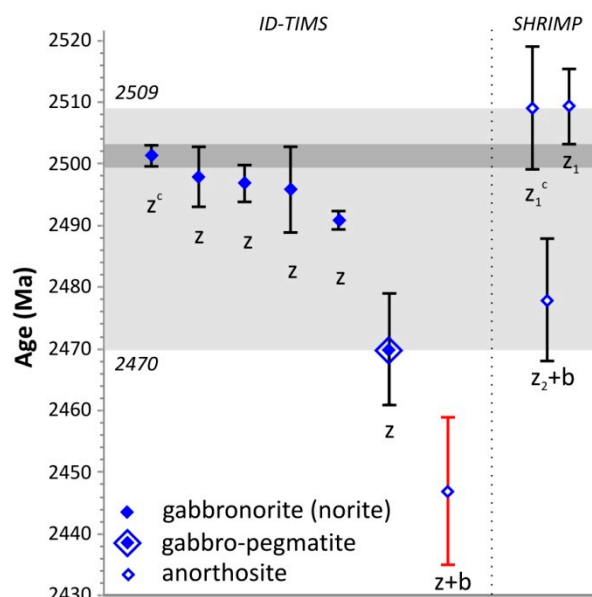
Figure 8. Overview of published U-Pb zircon (z) and baddeleyite (b) ages from different West-Pana lithologies. See Table 2 for references; C, mean $^{207}Pb/^{206}Pb$ age or concordia age. Note that the upper intercept age for magmatic zircon (z_1) from the Main Anorthosite Layer (2509.4 ± 6.2 Ma) is older than the mean $^{207}Pb/^{206}Pb$ age of the lower part of the intrusion (2501.5 ± 1.7 Ma, dark grey field), potentially indicating that (1) the upper portion of the intrusion is older than the lower portion and (2) the previous ID-TIMS date for this lithological unit (red error bar) did not record the actual crystallization age.

In terms of the crystallization history of the West-Pana intrusion and its long duration based on available age dating (Figure 8), this study shows that the geochronological questions are currently far from being conclusively answered. More modern and reliable high-precision age dating is needed to be able to resolve the entire crystallization history of not only the West-Pana intrusion, but the Fedorova-Pana Complex as a whole (Table 2, Figure 8). Considering the results of this study, the 2470 ± 9 Ma age for the gabbro-pegmatite from the LLH should be regarded as an upper temporal boundary for the crystallization of the intrusion (Figure 8). It appears, however, that this age most likely records the timing of late- to post-magmatic overprinting rather than the actual timing of emplacement, taking into account that high-precision dating of other large layered intrusions, such as the Bushveld or Stillwater Complexes, suggest a much shorter duration of magmatism, lasting for a few million years at most [15,42].

The main challenge associated with establishing a sound geochronological emplacement history for the Fedorova-Pana Complex is the precise dating of different mineralized and unmineralized lithologies from the Fedorova Tundra, the Northern Kamennik, and the Kievey deposits using the same methodology. This may potentially show that all these PGE deposits belong to the same mineral system and that they formed at the same time. These types of studies are necessary and feasible as was demonstrated for the PGE deposits of the Bushveld [15,43] and Stillwater Complexes [44].

5.2. Implications for the Formation of the South Reef

The formation of the South Reef PGE mineralization hosted in the uppermost portions of the Main Anorthosite Layer is one of the most important unresolved issues associated with the Fedorova-Pana Complex. Immediately after the discovery of mineralized rocks, containing tens of ppm Pd, the South Reef was considered to be highly prospective for further exploration [8]. Additional work on the South Reef, however, showed that the continuity of the high-grade PGE mineralization was generally limited to a few meters along strike of the Main Anorthosite Layer (cf. Boreholes 26 and 29 in Figure 3).

Based on the notion that the anorthosites in the West-Pana intrusion represented late sill-like bodies [13,36] and the presence of PGE-enriched rocks in the overlying and underlying gabbronoritic units [12], it was assumed that the PGEs were derived from the older gabbronorites that initially contained low-grade PGE mineralization. Upon intrusion of the anorthosites, this low-grade PGE mineralization was assimilated and enriched in the uppermost portions of the Main Anorthosite Layer [37].

The results of this study indicate that the anorthosites likely represent a regular part of the stratigraphy of West-Pana rather than late sill-like intrusions. This is further supported by the gradational lower contact of the anorthosite layer, which is characterized by progressively-increasing modal abundances of plagioclase (Figure 4B). Moreover, the anorthite content of cumulus plagioclase from the host gabbronorites and the anorthosite ranges from 73–75 mol. %, showing little variation across the contact [9]. It appears that the underlying gabbronorites together with the anorthosite represent the same cyclic unit of the ULH, while the overlying gabbronorites defines the base of another cyclic unit. The most likely source of the high-grade PGE mineralization hosted by the South Reef is the overlying gabbronoritic unit, which contains low-grade PGE mineralization associated with hornfels xenoliths, inequigranular gabbronorites, and norites. Two processes can be envisaged as potential mechanisms for the concentration of PGE in the anorthosite layer: (1) downward percolation of sulfide liquid from the overlying gabbronoritic magma into the uppermost portion of the anorthosite layer or (2) secondary redistribution of PGEs, which may coincide with the younger ages recorded by post-magmatic zircon and baddeleyite. The typical magmatic sulfide assemblage and the relatively high IPGE/PPGE ratios, however, argue strongly against a secondary origin of the mineralization.

Assuming that the most significant PGE enrichments in the Kola Region are associated with additional intrusions of sulfide-saturated and somewhat PGE-enriched magmas, as suggested for the Monchegorsk Complex [45,46] and the Fedorova intrusion [1], it is likely that the gabbronorites, overlying the Main Anorthosite Layer, also formed as a result of a late-stage intrusion of sulfide-saturated, PGE-enriched magma into the pre-existing cumulate pile. Further evidence for this mechanism is provided by the presence of a thin, discontinuous norite layer, as well as abundant hornfels xenoliths directly above the anorthosite layer (Figure 3). This late-stage intrusion may have led to the infiltration of PGE-enriched sulfide melt into the interstitial space of the underlying anorthosite cumulates [47,48], somewhat similar to contact-style sulfide mineralization, infiltrating basement lithologies that are in direct contact with the intrusion [46,49].

6. Concluding Remarks

The mineralized Main Anorthosite Layer is a plagioclase-rich cumulate that belongs to the cyclical Upper Layered Horizon of the West-Pana intrusion. The layer representing a leucocratic part of the cycle is overlain by slightly PGE-enriched gabbronorites of the next cyclic unit, which is characterized by abundant hornfels xenoliths and a discontinuous basal norite layer.

U-Pb SHRIMP-II dating of magmatic zircon with relatively high Th/U (0.9 to 3.7) from the anorthosite layer gives an upper intercept age of 2509.4 ± 6.2 Ma (2σ) and a concordia age of 2509 ± 10 Ma. The anorthosite and the related rocks of the Upper Layered Horizon are generally older than the lower portions of the West-Pana intrusion, suggesting an out-of-sequence emplacement of the intrusion. Secondary baddeleyite and zircon with relatively low Th/U (0.1–0.9) from the same anorthosite layer that were previously analyzed by multi-grain ID-TIMS yielded a significantly

younger age of 2476 ± 13 Ma. Our study indicates that this age does not record the actual timing of emplacement, but a secondary, post-magmatic alteration event.

References

1. Schissel, D.; Tsvetkov, A.A.; Mitrofanov, F.P.; Korchagin, A.U. Basal Platinum-Group Element Mineralization in the Federov Pansky Layered Mafic Intrusion, Kola Peninsula, Russia. *Econ. Geol.* **2002**, *97*, 1657–1677. [CrossRef]

2. Korchagin, A.U.; Subbotin, V.V.; Mitrofanov, F.P.; Mineev, S.D. Kievey PGE-Bearing Deposit in the West-Pana Layered Intrusion. *Strat. Min. Resour. Lapland Apatity* **2009**, *2*, 12–32.

3. Korchagin, A.U.; Goncharov, Y.V.; Subbotin, V.V.; Groshev, N.Y.; Gabov, D.A.; Ivanov, A.N.; Savchenko, Y.E. Geology and Composition of the Ores of the Low-Sulfide North Kamennik PGE Deposit in the West-Pana Intrusion. *Ores Met.* **2016**, *1*, 42–51. (In Russian)

4. Kazanov, O.V.; Kalinin, A. The Structure and PGE Mineralization of the East Pansky Layered Massif. *Strat. Min. Resour. Lapland-Base Sustain. Dev. North. Interreg-Tacis Proj. Apatity Russ.* **2008**, *1*, 57–68.

5. Rasilainen, K.; Eilu, P.; Halkoaho, T.; Iljina, M.; Karinen, T. Quantitative Mineral Resource Assessment of Undiscovered PGE Resources in Finland. *Ore Geol. Rev.* **2010**, *38*, 270–287. [CrossRef]

6. Gurskaya, L.I.; Dodin, D.A. Mineral Resources of Platinum Group Metals in Russia: Expansion Prospects. *Reg. Geol. Met.* **2015**, *64*, 84–93. (In Russian)

7. Balabonin, N.L.; Korchagin, A.U.; Latypov, R.M.; Subbotin, V.V. Fedorovo-Pansky Intrusion. In *Kola Belt of Layered Intrusions. Geological Institute Kola Science Centre, Russian Academy of Sciences, Apatity, 7th International Platinum Symposium. Guide to the Pre-Symposium Field Trip*; KSC RAS: Apatity, Russia, 1994; pp. 9–41.

8. Mitrofanov, F.P.; Korchagin, A.U.; Dudkin, K.O.; Rundkvist, T.V. Fedorova-Pana Layered Mafic Intrusion (Kola Peninsula, Russia): Approaches, Methods, and Criteria for Prospecting PGEs. In *Exploration for Platinum-Group Elements Deposits*; Short Course Delivered on Behalf of the Mineralogical Association of Canada in Oulu, Finland; University of Toronto: Toronto, ON, Canada, 2005; Volume 35, pp. 343–358.

9. Groshev, N.Y.; Borisenko, Y.S.; Savchenko, Y.E. Plagioclase Composition through the Section of the Main Anorthosite Layer of the West-Pana Massif (Kola Peninsula, Russia): New Data. *Vestn. KSC* **2017**, *1*, 1–15. (In Russian)

10. Subbotin, V.V.; Korchagin, A.U.; Savchenko, E.E. Platinum Mineralization of the Fedorova-Pana Ore Node: Types of Ores, Mineral Compositions and Genetic Features. *Vestn. KSC* **2012**, *1*, 54–65. (In Russian)

11. Chernyavsky, A.V.; Groshev, N.Y.; Korchagin, A.U.; Shilovskikh, V.V. Minerals of Platinum Group Elements through the South Reef, West-Pana Intrusion. *Tr. FNS* **2018**, *15*, 392–395. (In Russian) [CrossRef]

12. Karpov, S.M. Geological Structure of the Pana Intrusion and Features of Localization of Complex PGE Mineralization. Ph.D. Thesis, KSC RAS, Apatity, Russia, 2004. (In Russian)

13. Bayanova, T.; Ludden, J.; Mitrofanov, F. Timing and Duration of Palaeoproterozoic Events Producing Ore-Bearing Layered Intrusions of the Baltic Shield: Metallogenic, Petrological and Geodynamic Implications. *Geol. Soc. Lond. Spec. Publ.* **2010**, *323*, 165–198. [CrossRef]

14. Mitrofanov, F.P.; Bayanova, T.B.; Korchagin, A.U.; Groshev, N.Y.; Malitch, K.N.; Zhirov, D.V.; Mitrofanov, A.F. East Scandinavian and Noril'sk Plume Mafic Large Igneous Provinces of Pd-Pt Ores: Geological and Metallogenic Comparison. *Geol. Ore Depos.* **2013**, *55*, 305–319. [CrossRef]

15. Zeh, A.; Ovtcharova, M.; Wilson, A.H.; Schaltegger, U. The Bushveld Complex Was Emplaced and Cooled in Less than One Million Years—Results of Zirconology, and Geotectonic Implications. *Earth Planet. Sci. Lett.* **2015**, *418*, 103–114. [CrossRef]

16. Amelin, Y.V.; Heaman, L.M.; Semenov, V.S. U-Pb Geochronology of Layered Mafic Intrusions in the Eastern Baltic Shield: Implications for the Timing and Duration of Paleoproterozoic Continental Rifting. *Precambrian Res.* **1995**, *75*, 31–46. [CrossRef]

17. Dokuchaeva, V.S. Petrology and Ore Genesis in the Federov Pansky Intrusion. *Geol. Genes. Platin.-Gr. Met. Depos. Mosc. Nauk. Publ. House* **1994**, *1*, 87–100. (In Russian)

18. Odinets, A.Y. The Petrology of the Pansky Massif of Mafic Rocks, Kola Peninsula. Ph.D. Thesis, Kola Branch AS USSR, Apatity, USSR, 1971. (In Russian)

19. Kozlov, E.K. *Natural Series of Nickel-Bearing Intrusion Rocks and Their Metallogeny*; Nauka: Leningrad, USSR, 1973. (In Russian)

20. Staritsina, G.N. Fedorova Tundra Massif of Basic-Ultrabasic Rocks. In *Issues of Geology and Mineralogy, Kola Peninsula*; Kola Branch AS USSR: Apatity, Russia, 1978; pp. 50–91. (In Russian)

21. Latypov, R.M.; Chistyakova, S.Y. *Mechanism of Differentiation of the West Pansky Tundra Layered Intrusion*; Kola Science Center: Apatity, Russia, 2000. (In Russian)

22. Latypov, R.M.; Mitrofanov, F.P.; Skiba, V.I.; Alapieti, T.T. The Western Pansky Tundra Layered Intrusion, Kola Peninsula: Differentiation Mechanism and Solidification Sequence. *Petrology* **2001**, *9*, 214–251.

23. Latypov, R.M.; Mitrofanov, F.P.; Alapieti, T.T.; Halkoaho, T.A.A. Petrology of the Lower Layered Horizon of the Western Pansky Tundra Intrusion, Kola Peninsula. *Petrology* **1999**, *7*, 482–508.

24. Korchagin, A.U.; Subbotin, V.V.; Mitrofanov, F.P.; Mineev, S.D. Kievey PGE-Bearing Deposit of the West-Pana Layered Intrusion: Geological Structure and Ore Composition. In *Strategic Mineral Resources of Lapland—Base for the Sustainable Development of the North*; KSC RAS: Apatity, Russia, 2009; pp. 12–33.

25. Latypov, R.M.; Chistyakova, S.Y. Physicochemical Aspects of Magnetite Gabbro Formation in the Layered Intrusion of the Western Pansky Tundra, Kola Peninsula, Russia. *Petrology* **2001**, *9*, 25–45.

26. Latypov, R.M.; Mitrofanov, F.P.; Alapieti, T.T.; Kaukonen, R.J. Petrology of the Upper Layered Horizon of the West-Pansky Tundra Intrusion (Kola Peninsula, Russia). *Geol. I Geofiz.* **1999**, *40*, 1434–1456.

27. Groshev, N.Y.; Rundkvist, T.V.; Bazay, A.V. Find of Cordierite Hornfels in the Upper Layered Horizon of the West-Pana Intrusion, Kola Peninsula. *Zap. RMO* **2015**, *144*, 82–98.

28. Subbotin, V.V.; Korchagin, A.U.; Savchenko, E.E. PGE Mineralization of the Fedorova-Pana Ore Complex: Types of Mineralization, Mineral Composition, Features of Genesis. *Her. Kola Sci. Cent. RAS* **2012**, *1*, 55–66.

29. Groshev, N.Y. Plagioclase Composition as an Indicator of the Economic Potential of a PGE Reef in a Layered Basic Intrusion. *Tr. FNS* **2017**, *14*, 86–88.

30. Subbotin, V.V.; Korchagin, A.U.; Gabov, D.A.; Savchenko, E.E. Localization and Composition of Low-Sulfide PGE Mineralization in the West-Pana Intrusion. *Tr. FNS* **2012**, *9*, 302–307.

31. Bayanova, T.B. *Age of Reference Geological Complexes of the Kola Region and Duration of Magmatic Processes*; Nauka: St. Petersburg, Russia, 2004.

32. Williams, I.S. U-Th-Pb Geochronology by Ion Microprobe. *Rev. Econ. Geol.* **1998**, *7*, 1–35.

33. Schuth, S.; Gornyy, V.; Berndt, J.; Shevchenko, S.; Sergeev, S.; Karpuzov, A.; Mansfeld, T. Early Proterozoic U-Pb Zircon Ages from Basement Gneiss at the Solovetsky Archipelago, White Sea, Russia. *Int. J. Geosci.* **2012**, *03*, 289–296. [CrossRef]

34. Stacey, J.S.; Kramers, J.D. Approximation of Terrestrial Lead Isotope Evolution by a Two-Stage Model. *Earth Planet. Sci. Lett.* **1975**, *26*, 207–221. [CrossRef]

35. Ludwig, K.R. *User's Manual for Isoplot 3.75: A Geochronological Toolkit for Microsoft Excel*; Berkeley Geochronology Center: Berkeley, CA, USA, 2012.

36. Heaman, L.M.; LeCheminant, A.N. Paragenesis and U-Pb Systematics of Baddeleyite (ZrO_2). *Chem. Geol.* **1993**, *110*, 95–126. [CrossRef]

37. Chashchin, V.V.; Mitrofanov, F.P. The Paleoproterozoic Imandra-Varzuga Rifting Structure (Kola Peninsula): Intrusive Magmatism and Mineralogy. *Geodin. I Tektonofiz.* **2015**, *5*, 231–256. [CrossRef]

38. Nitkina, E.A. U-Pb Zircon Dating of Rocks of the Platiniferous Fedorova-Pana Layered Massif, Kola Peninsula. *Dokl. Earth Sci.* **2006**, *408*, 551–554. [CrossRef]

39. Groshev, N.Y.; Nitkina, E.A.; Mitrofanov, F.P. Two-Phase Mechanism of the Formation of Platinum-Metal Basites of the Fedorova Tundra Intrusion on the Kola Peninsula: New Data on Geology and Isotope Geochronology. *Dokl. Earth Sci.* **2009**, *427*, 1012–1016. [CrossRef]

40. Balashov, Y.A.; Bayanova, T.B.; Mitrofanov, F.P. Isotope Data on the Age and Genesis of Layered Basic-Ultrabasic Intrusions in the Kola Peninsula and Northern Karelia, Northeastern Baltic Shield. *Precambrian Res.* **1993**, *64*, 197–205. [CrossRef]

41. Bayanova, T.B.; Rundquist, T.V.; Serov, P.A.; Korchagin, A.U.; Karpov, S.M. The Paleoproterozoic Fedorov-Pana Layered PGE Complex of the Northeastern Baltic Shield, Arctic Region: New U-Pb (Baddeleyite) and Sm-Nd (Sulfide) Data. *Dokl. Earth Sci.* **2017**, *472*, 1–5. [CrossRef]

42. Wall, C.J.; Scoates, J.S.; Weis, D.; Friedman, R.M.; Amini, M.; Meurer, W.P. The Stillwater Complex: Integrating Zircon Geochronological and Geochemical Constraints on the Age, Emplacement History and Crystallization of a Large, Open-System Layered Intrusion. *J. Pet.* **2018**, *59*, 153–190. [CrossRef]

43. Scoates, J.S.; Friedman, R.M. Precise Age of the Platiniferous Merensky Reef, Bushveld Complex, South Africa, by the U-Pb Zircon Chemical Abrasion ID-TIMS Technique. *Econ. Geol.* **2008**, *103*, 465–471. [CrossRef]

44. Wall, C.J.; Scoates, J.S. High-Precision U-Pb Zircon-Baddeleyite Dating of the JM Reef Platinum Group Element Deposit in the Stillwater Complex, Montana (USA). *Econ. Geol.* **2016**, *111*, 771–782. [CrossRef]

45. Karykowski, B.T.; Maier, W.D.; Groshev, N.Y.; Barnes, S.J.; Pripachkin, P.V.; McDonald, I. Origin of Reef-Style Pge Mineralization in the Paleoproterozoic Monchegorsk Complex, Kola Region, Russia. *Econ. Geol.* **2018**, *113*, 1333–1358. [CrossRef]

46. Karykowski, B.T.; Maier, W.D.; Groshev, N.Y.; Barnes, S.J.; Pripachkin, P.V.; McDonald, I.; Savard, D. Critical Controls on the Formation of Contact-Style PGE-Ni-Cu Mineralization: Evidence from the Paleoproterozoic Monchegorsk Complex, Kola Region, Russia. *Econ. Geol.* **2018**, *113*, 911–935. [CrossRef]

47. Karykowski, B.T.; Maier, W.D. Microtextural Characterisation of the Lower Zone in the Western Limb of the Bushveld Complex, South Africa: Evidence for Extensive Melt Migration within a Sill Complex. *Contrib. Miner. Pet.* **2017**, *172*, 1–18. [CrossRef]

48. Ivanov, A.N.; Groshev, N.Y.; Korchagin, A.U. Transgressive Structures of the Lower Layered Horizon in the Area of North Kamennik Low-Sulfide PGE Deposit. *Tr. FNS* **2018**, *15*, 124–127. [CrossRef]

49. Groshev, N.Y.; Pripachkin, P.V. Geological setting and platinum potential of the Gabbro-10 massif, Monchegorsk Complex, Kola Region. *Ores Met.* **2018**, *4*, 4–13. [CrossRef]